Journal of Applied Physics

RESEARCH ARTICLE | JANUARY 02 2024

Unravelling the doping mechanism and origin of carrier limitation in Ti-doped In_2O_3 films

Special Collection: Native Defects, Impurities and the Electronic Structure of Compound Semiconductors: A Tribute to Dr. Wladyslaw Walukiewicz

Ann-Katrin Emmerich ; Kim Alexander Creutz; Yaw-Yeu Cheng ; Jean-Christophe Jaud; Andreas Hubmann ; Andreas Klein

J. Appl. Phys. 135, 015101 (2024)
https://doi.org/10.1063/5.0175864

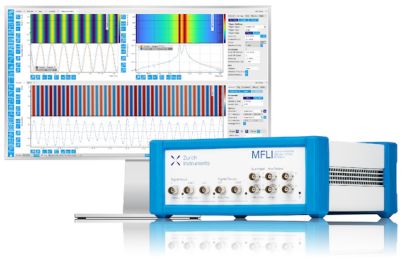

Journal of Applied Physics ARTICLE pubs.aip.org/aip/jap

Unravelling the doping mechanism and origin of carrier limitation in Ti-doped In_2O_3 films

Cite as: J. Appl. Phys. **135**, 015101 (2024); doi: 10.1063/5.0175864
Submitted: 9 September 2023 · Accepted: 10 December 2023 ·
Published Online: 2 January 2024

Ann-Katrin Emmerich, Kim Alexander Creutz, Yaw-Yeu Cheng, Jean-Christophe Jaud, Andreas Hubmann, and Andreas Klein[a)]

AFFILIATIONS

Institute of Materials Science, Technische Universität Darmstadt, Otto-Berndt-Str. 3, 64287 Darmstadt, Germany

Note: This paper is part of the Special Topic on Native Defects, Impurities and the Electronic Structure of Compound Semiconductors: A Tribute to Dr. Wladyslaw Walukiewicz.

[a)]**Author to whom correspondence should be addressed:** andreas.klein@tu-darmstadt.de

ABSTRACT

Ti-doped In_2O_3 thin films with varying Ti contents are prepared by partial reactive co-sputtering using ceramic In_2O_3 and metallic Ti targets and characterized by *in situ* x-ray photoelectron spectroscopy, electrical conductivity, and Hall-effect measurements. For a substrate temperature of 400 °C, the carrier concentration increases faster than the Ti content and saturates at $\approx 7.4 \times 10^{20}$ cm^{-3}. Based on these results, it is suggested that Ti does not directly act as donor in In_2O_3 but is rather forming TiO_2 precipitates and that the related scavenging of oxygen generates oxygen vacancies in In_2O_3 as origin of doping. Neutralization of oxygen vacancies is, therefore, suggested to be origin of the limitation of the carrier concentration in Ti-doped In_2O_3 films.

INTRODUCTION

Donor-doped In_2O_3 is a transparent conductive oxide, which is extensively used as an electrode material in solar cell and display technologies.[1,2] Improving the performance of those devices is a permanent goal of research and industry, which makes it indispensable to increase the conductivity and, hence, efficiency of doped In_2O_3. Therefore, understanding the electrical transport properties and the influences and limitations on them is crucial. The combination of high electrical conductivity and optical transparency is accomplished by degenerate doping of a wide-gap oxide semiconductor. In the case of In_2O_3, the optically forbidden transitions from the highest valence band states further reduce visible light absorption of thin films.[3] Highest electrical conductivities exceeding 10^4 S/cm are obtained with Sn as a donor species, reaching carrier concentrations exceeding 10^{21} cm^{-3}.[4–6] At such high carrier concentrations, the mobility of the electrons is limited by ionized impurity scattering, while grain boundary potential barriers limit the mobility of polycrystalline films for lower carrier concentrations.[5,7] Sn-doped In_2O_3 (ITO) films with highest conductivity suffer from a reduction of the transparency in the near infrared region. This is caused by excitation of collective vibrations of the electron gas causing light reflection.[8] For certain applications, for example, as an electrode in crystalline Si solar cells, the infrared reflectivity is undesirable, as it reduces photocurrent generation.[9] Transparency in the infrared region can be increased with higher carrier mobilities, which raise the plasmon wavelength. In_2O_3 thin films can exhibit substantially higher carrier mobilities with other dopants than Sn, such as Ti, Mo, W, Zr, and Ce.[10–17] High carrier mobilities have also been achieved by annealing In_2O_3 films deposited at room temperature with the addition of H_2O to the process gas.[18] This solid-phase crystallization process leads to large grain sizes and can also be applied in combination with other donor dopants.[19]

As illustrated in Fig. 1, carrier mobilities >100 cm^2/Vs are only achieved for carrier concentrations $1 - 4 \times 10^{20}$ cm^{-3}. Despite the higher carrier mobilities obtained with other dopants, the highest conductivities are still obtained with Sn doping, which appears to be the only dopant allowing for carrier concentrations $>10^{21}$ cm^{-3}. Understanding the limitations of carrier concentrations may, therefore, help to further improve the electrical and optical properties of donor-doped In_2O_3 films. As introduced by

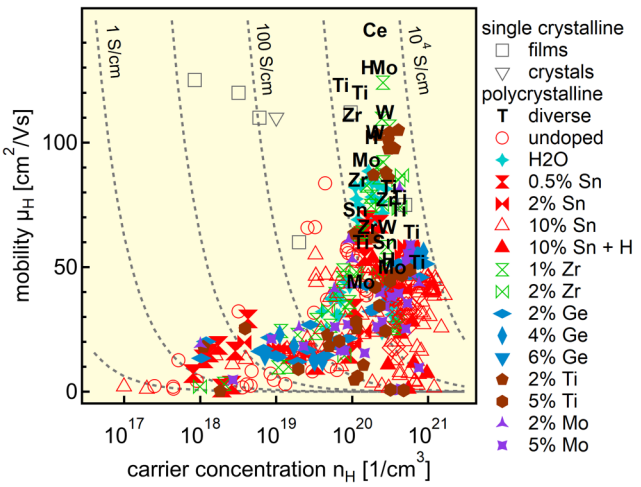

FIG. 1. Carrier mobility vs carrier concentration of differently doped In_2O_3 thin films. Colored symbols are thin films prepared with different dopants. Selected data from the literature are indicated by the dopant element.[4,10–17] The dashed lines correspond to constant electrical conductivity.

Frank and Köstlin, the carrier concentrations in highly Sn-doped In_2O_3 are limited by oxygen interstitials, which were suggested to compensate the Sn dopants by the formation of neutral $(2Sn_{In}O_i)^{\times}$ defect complexes.[20] The incorporation of oxygen interstitials was later confirmed by different authors[21,22] and related to the self-compensation mechanism.[23,24] Self-compensation is induced by the decrease of the formation energy of oxygen interstitial defects with increasing Fermi energy.[25] However, as long as the association energies between the different dopants and oxygen interstitials are comparable, self-compensation should be independent on the dopant species and result in a similar limitation of carrier concentration. According to the different carrier concentrations achieved with different dopants (see Fig. 1), this does not seem to be the case. Therefore, other mechanisms limiting the Fermi energy are expected to play a role.[26] Here, two different mechanisms are considered to limit the carrier concentrations in donor-doped In_2O_3: (i) the charge transition level of the dopant[23] and (ii) segregation of the dopants.[7] The latter is associated with the formation enthalpy of the dopants, which increases with increasing Fermi energy.[23]

In this work, the limitation of the carrier concentration in Ti-doped In_2O_3 was studied by means of *in situ* x-ray photoelectron spectroscopy (XPS), conductivity, and Hall-effect measurements. Carrier mobilities of $>100\ cm^2/Vs$ have been demonstrated in the literature, but the carrier concentrations did not exceed $7.1 \times 10^{20}\ cm^{-3}$.[10,11,16]

EXPERIMENTAL

In order to account for the potential limitation of carrier concentration by oxygen interstitials, we have prepared our films using partial reactive co-sputtering. The configuration is illustrated in Fig. 2 (right), where ceramic In_2O_3 and a metallic Ti target are installed. By variation of the sputter power and the distances between the targets and the substrate, it is possible to control not only the Ti content in the films but also the oxygen content in the process gas and in the films. In order to lower the amount of oxygen interstitials, the effective oxygen partial pressure in the

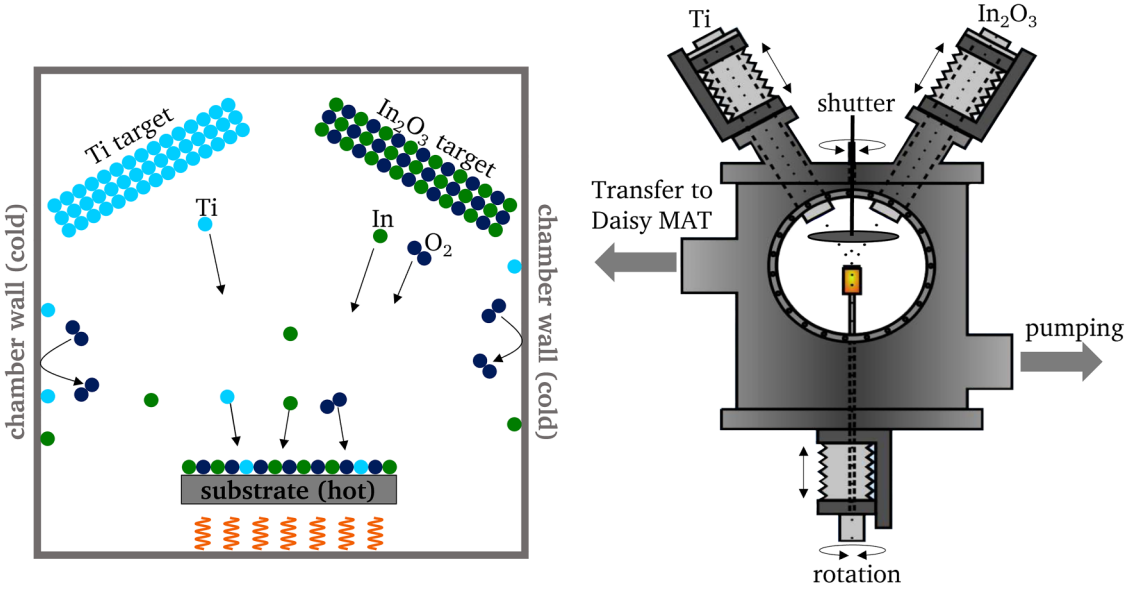

FIG. 2. Schematic setup of the partial reactive co-sputtering arrangement (left) and layout of the used co-sputtering chamber (right). The distances between the In_2O_3 and the Ti target to the rotating sample holder can be varied independently.

chamber during deposition needs to be lowered toward the thermodynamic stability limit of In_2O_3. This is generally difficult during sputtering from ceramic targets. As illustrated in Fig. 2 (left), metal atoms emitted from the target either reach the substrate or stick to the (unheated) chamber walls (the sticking coefficient of metal atoms is expected to be 1), while the less reactive O_2 molecules emitted from the target are expected to have a sticking coefficient lower than 1.[27,28] Therefore, the ratio of oxygen to metal species in the process gas is larger than in the target. The partial co-sputtering approach facilitates lower oxygen content in the process gas in two ways. First, as the In_2O_3 target is not doped, it contains no oxygen interstitials and, therefore, less oxygen than a doped target. Second, dopant atoms not arriving on the substrate will stick to the chamber wall and bind oxygen atoms from the process gas. This effect is used in vacuum technology to achieve ultrahigh vacuum conditions. It is particularly the evaporation of Ti, which is used for this purpose in titanium sublimation pumps.[29,30]

The deposition of the thin films as well as the characterization with XPS were performed in the Darmstadt Integrated System for Materials Research (DAISY-MAT[31]). For co-sputtering, a 99.999% pure indium oxide target (Evochem, Offenbach am Main, Germany) and a 99.99% pure titanium target (Alineason, Frankfurt am Main, Germany) were used. All depositions were carried out at a chamber pressure of 0.5 Pa in a pure argon atmosphere with 13.56 MHz radio frequency plasma excitation. The Ti content in the films was varied by adjusting the distance between the titanium target and the substrate and by changing the RF power applied to the titanium target. The substrate temperature during the deposition was set between room temperature and 400 °C. Heating and cooling were performed with a rate of $10-15$ K/min in the process gas. Before each deposition, both targets were pre-sputtered for at least 5 min with a closed shutter. To ensure homogeneous film composition and thickness, the sample was rotated along the vertical axis during deposition. Fused silica substrates with a 10×10 mm^2 dimension were used for all depositions. Before deposition, the corners of the substrate were coated with platinum to establish the electrical contact between the sample holder and the film for XPS analysis and for electrical measurements. For comparison, films were also deposited by magnetron sputtering with varying Ar/O_2 gas composition using In_2O_3 targets doped with 2 mol. % and with 5 mol. % Ti (Alineason, Frankfurt am Main, Germany). In all cases, deposition times were adjusted to result in film thickness of $300-400$ nm.

Photoelectron spectroscopy was carried out without breaking vacuum directly after deposition using a Physical Electronics PHI 5700 photoelectron spectrometer system (Physical Electronics, Chanhassen, MI) with monochromatic Al Kα excitation. Binding energies were measured against the Fermi energy, which was calibrated using a sputter cleaned silver standard on a daily basis. For the determination of peak intensities, background subtraction was done using a Shirley function for the In $3d$ and O $1s$ emissions. Due to the low Ti content and the location of the Ti $2p$ emission on the high binding energy tail of the In $3d_{5/2}$ component, background subtraction of the Ti $2p_{3/2}$ emission was performed using a higher order polynomial. The composition of the sample was finally determined using integrated peak intensities and sensitivity factors provided by the manufacturer of the spectrometer system.[32] In order to assess potential surface segregation of Ti, sputter depth profiles were carried out. Ion etching for depth profiling was performed with 1 keV Ar ions leading to an etching rate of $\approx$1 nm/min.

Electrical conductivity and Hall-effect measurements were performed in a homemade setup[33,34] at room temperature. All measurements were done with the van der Pauw geometry. Current voltage tests were carried out beforehand to evaluate contact properties and to fix the measurement currents. Magnetic fields of 1.3 T were applied for Hall-effect measurements. Reported data are averages of at least ten measurements. The standard deviation of the different measurements remained $<3\%$. Optical properties in the wavelength range of $200-2500$ nm were characterized using an Agilent Cary 7000 Spectrophotometer (Agilent Technologies, Santa Clara, CA), equipped with a deuterium and halogen lamp for the UV and for the visible to near infrared range, respectively. The transmittance was recorded with an incident angle of 6° for s and p polarized light. A baseline of air was measured once a day and subtracted from the data.

RESULTS

X-ray diffraction

X-ray diffractograms of Ti-doped films are presented in Fig. 3. The broad feature at low diffraction angles is attributed to the amorphous quartz glass substrate. All diffraction peaks match the

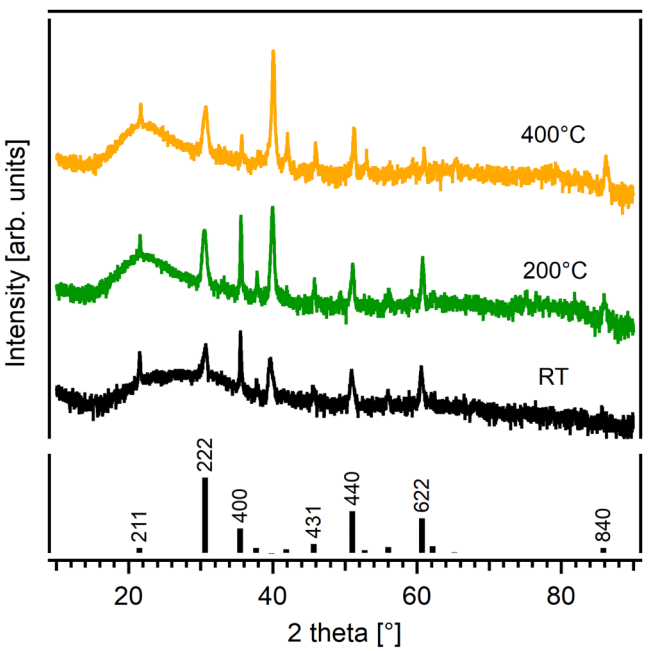

FIG. 3. X-ray diffractogram of films deposited at room temperature, at 200 °C, and at 400 °C. The black bars at the bottom indicate the peak positions and relative intensities of bixbyite indium oxide (ICCD pattern: 00-006-0416).

diffraction data of cubic In_2O_3 (ICDD: 00-006-0416). No diffraction peaks related to TiO, TiO_2, or Ti_2O_3 can be identified. However, it cannot be excluded that the peaks labeled as (222) and (332) in the diffractogram of the sample deposited at 400 °C contain contributions of an In_2TiO_5 phase.[11]

Photoelectron spectroscopy

XP survey spectra of films deposited at room temperature, 200 °C, and 400 °C are displayed in Fig. 4. It can be noticed that only In and O signals are observed. The absence of contaminations and impurities is indispensable for the detailed analysis of sample composition and electrical properties performed in this work. For each temperature, films grown with and without Ti are included. There are no significant differences between the spectra. Only In and O related emissions can be clearly discerned. The Ti 2*p* emission, which is the most intense signal related to titanium, is barely visible in the spectra, although the Ti content is up to 10 mol. %. This is related to the small difference in binding energy between the Ti 2*p* peak at ≈458 eV and the In 3*d* emission. The Ti 2*p* peak also has a significantly lower photoionization cross section as compared to the In 3*d* emission, further reducing its intensity.[35]

X-ray photoelectron core level spectra of In_2O_3 films grown at 400 °C with different amounts of Ti are presented in Fig. 5. The spectra of the films deposited at room temperature and at 200 °C are very similar and not included in the figure but shown in the supplementary material. The O 1*s* emission of the nominally undoped In_2O_3 films exhibits a slight asymmetry toward higher binding energy and an additional peak with low intensity at a binding energy of ≈532.5 eV. The asymmetry can be related to the high carrier concentration of the film.[36,37] The small high binding energy peak, which is frequently observed by *in situ* XPS analysis of magnetron sputtered and of reactively evaporated films,[38,39] may originate from adsorbed oxygen species. According to *ab initio* calculations, oxygen dimer species are likely present at surfaces of undoped In_2O_3[40,41] supporting such an assignment. When Ti is added to the deposition, the binding energy of the O 1*s* peak and the asymmetry of the peak are increasing. Both correspond with an increasing carrier concentration. The In 3*d* emission shows similar changes. The asymmetry and the binding energy also increase with increasing Ti content. The onset of the valence band spectra, which is at ≈3 eV binding energy, also increases with the addition of Ti. Moreover, the valence band peak at ≈4 eV decreases. This indicates lowering of the oxygen content in the films,[37] which has been intended by the addition of Ti. The lower oxygen content in the film is further indicated by the increasing intensity of bandgap emissions (see horizontal black lines in Fig. 5).[42] However, the In 3*d* peaks confirm that no metallic In species are observed. Therefore, the reduction of the oxygen content is not strong enough to destabilize the In_2O_3 phase.

The Ti 2*p* spectra of films deposited at different substrate temperatures with different Ti content are displayed in Fig. 6. Only samples with Ti content >3 cat. % are presented. Nevertheless, the Ti content could be quantified down to a level of ≈0.5 cat. % when the recording times were sufficiently increased. To demonstrate

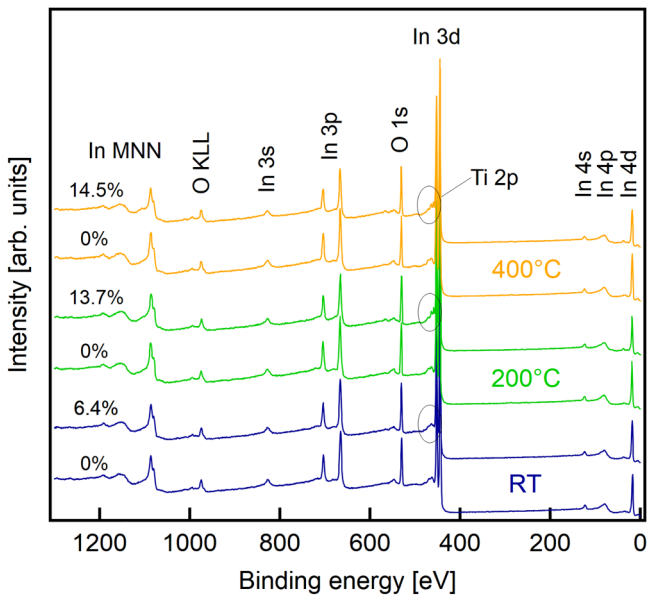

FIG. 4. X-ray photoelectron survey spectra of In_2O_3 films grown at different substrate temperatures deposited without and with Ti. The Ti 2*p* signal is barely observable as indicated by the circles. The numbers indicate the Ti content in cation percent.

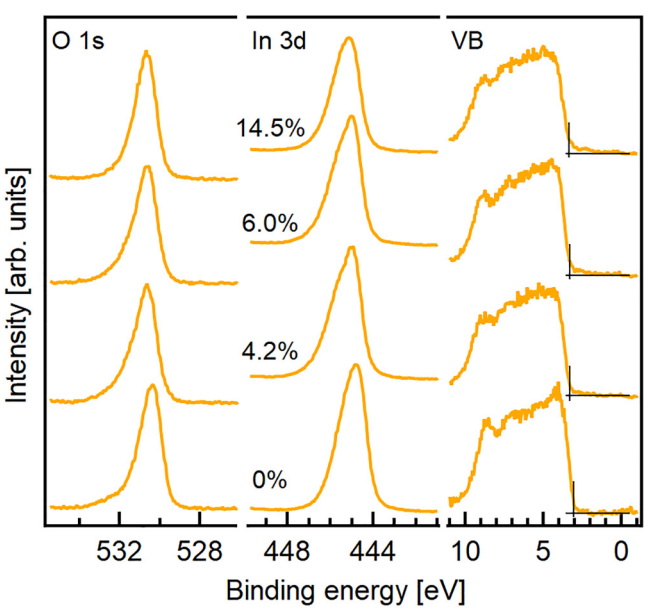

FIG. 5. X-ray photoelectron core level and valence band spectra of In_2O_3 films grown at 400 °C with different Ti content. The Ti content is indicated at the spectra in cation %. The position of the valence band maxima has been determined by the intersection of the linearly extrapolated leading edge of the valence bands and the background lines and are indicated by black vertical lines. The black horizontal lines are included to emphasize the increase of the bandgap emissions with increasing Ti content.

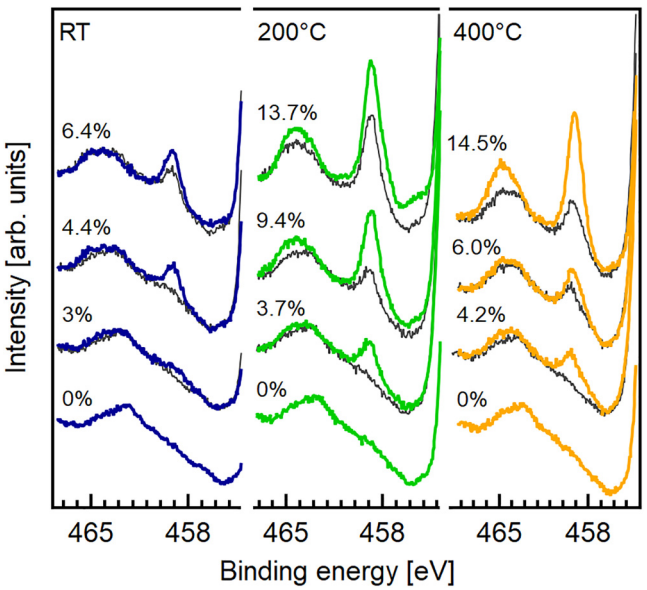

FIG. 6. Selected Ti 2*p* core level spectra of Ti-doped In_2O_3 films grown at different substrate temperatures. The extracted concentration of Ti is indicated at the spectra in cation %. The spectra shown in gray thin lines correspond to those with the lower Ti content to illustrate the evolution of the spectra with increasing Ti content.

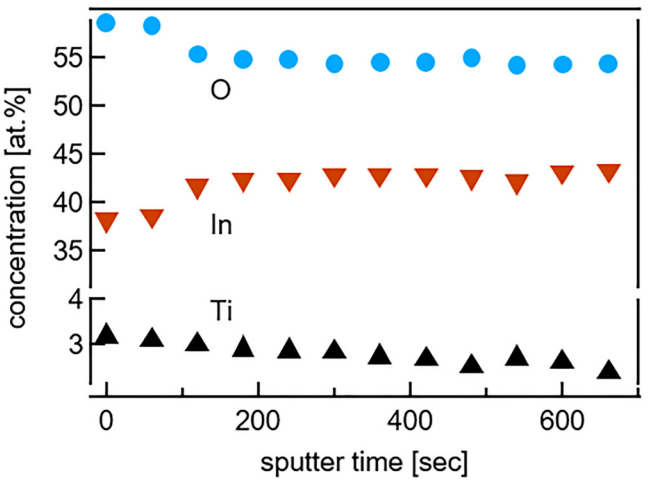

FIG. 7. Composition of a co-sputtered Ti-doped In_2O_3 film recorded in the course of Ar ion etching. The Ti-content of the film decreases from 3.2 at. % (≈8 cat.%) to 2.4 at. % in the course of etching time.

this, Ti 2*p* core level spectra down to the lowest Ti contents are illustrated in Fig. S1 of the supplementary material. The maximum of the Ti $2p_{3/2}$ emission is located at ≈459 eV in all cases, clearly indicating a dominant Ti^{4+} oxidation state. The Ti $2p_{3/2}$ emissions of the films grown at room temperature are also rather symmetric, providing no evidence for the existence of substantial amounts of reduced Ti^{3+} species. The situation is less clear for the films grown at a higher temperature. This is partially related to the higher binding energy and the stronger asymmetry of the neighboring In 3*d* emission, which is a result of the higher carrier concentrations of these films. Consequently, the presence of Ti^{3+} species cannot be completely excluded for these films. Nevertheless, the spectra confirm a dominant Ti^{4+} oxidation state and that the relative amount Ti^{3+} does not increase with increasing Ti content. This has to be expected if the neutralization of the Ti dopants would limit the carrier concentration at higher Ti concentration.

The dominant 4+ oxidation state of Ti could also be caused by the formation of a TiO_2 phase at the surface. Such segregation of dopants has been observed for Sn-doped In_2O_3[7] and also for Ti-doped films deposited from Ti-doped targets.[43] The latter is only pronounced at a deposition temperature of 600 °C. In these cases, the formation of a TiO_2 surface phase can be revealed by comparing the Ti content extracted in the XP spectra to the nominal target composition, which corresponds to the bulk composition. In the case of ITO films, the observed segregation of Sn under reducing conditions has further been confirmed to change reversibly with the atmosphere.[37] In the case of the co-sputtered Ti-doped films, the bulk composition is not known. Therefore, a sputter depth profile was performed on a sample with a titanium content of ≈8 cat. % (3.2 at. %). The evolution of the composition is depicted in Fig. 7. With increasing sputter time, the titanium content decreases from 3.2 to 2.4 at.%. The rather small decrease of the Ti content indicates that the majority of the Ti atoms are present inside the films and not at the surface. It is not likely that the In:Ti ratio is affected by Ar ion etching. First of all, the oxygen content remains well above the oxygen content of 50%, at which metallic In is formed. Moreover, no Ti^{3+} is formed during depth profiling. For Sn-doped In_2O_3, we have also not observed a change of the dopant content upon Ar ion etching with the given parameters (1 keV Ar ions).

Electrical properties

The results of the Hall-effect and conductivity measurements of the samples deposited at room temperature, 200, and 400 °C are summarized in Fig. 8. Panels (a)–(c) display the carrier concentration, mobility, and conductivity as a function of the Ti-content determined by XPS. Panel (d) depicts the mobility as a function of the carrier concentration of co-sputtered samples. Data from various nominally undoped In_2O_3 films and of Ti-doped films prepared from In_2O_3 targets doped with 2 and 5 mol % Ti are included for comparison. We also included various data reported in the literature.[10,11,16]

The carrier concentration of the co-sputtered Ti-doped films increases with Ti content but does not exceed 7.4×10^{20} cm^{-3}. This value is slightly higher than the highest value of Ti-doped In_2O_3 films reported in the literature.[13] For a deposition temperature of 400 °C, the saturation of the carrier concentration is reached already at Ti content as low as ≈1 cat.%, corresponding to a Ti concentration of $\approx 3 \times 10^{20}$ cm^{-3}. This is only about one half of the electron concentration determined from Hall-effect measurements and suggests that every Ti atom is contributing two electrons

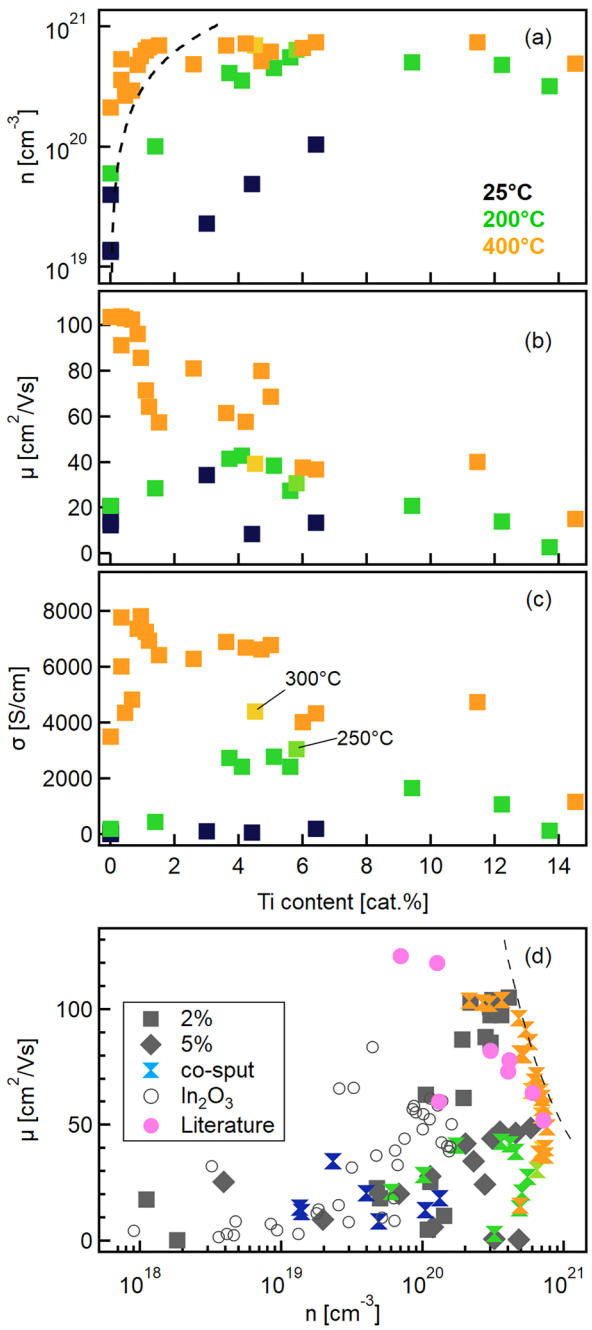

FIG. 8. Electrical properties of partially reactive co-sputtered Ti-doped In_2O_3 films. Panels (a)–(c) display the carrier concentration, mobility, and conductivity as a function of the Ti-content determined by XPS. Panel (d) presents the mobility vs the carrier concentration of the films, together with data from nominally undoped In_2O_3 films, from films prepared by sputtering from targets doped with 2 and 5 mol. % Ti, and from the literature.[10,11,16] The color coding of the co-sputtered films in (d) is the same as that in panels (a)–(c). The dashed line in (a) corresponds to an electron concentration equal to the Ti concentration and the dashed line in (d) to a conductivity of 7800 S/cm, respectively.

to the concentration of mobile carriers. The observation that the carrier concentration is exceeding the Ti concentration at low Ti content is emphasized in Fig. 8(a) by the dashed line, which represents an electron concentration equal to the Ti concentration.[44] For the films deposited at 400 °C, this is the case for all films with Ti concentrations <2 cat.%. The films deposited at a substrate temperature of 200 °C reach a similar maximum carrier concentration but at a Ti content of 6 cat.%. The different behavior is assigned to the lower crystallinity of the films.

High carrier mobilities >100 cm^2/Vs are only obtained at a deposition temperature of 400 °C and only for Ti contents <1 cat.%. For higher Ti content, the mobility gradually decreases to about 40 cm^2/Vs. This is also the highest mobility obtained for deposition at room temperature and 200 °C.

The highest conductivity slightly above 7800 S/cm is obtained for a Ti content of ≈1 cat.% at a carrier concentration of 5.7×10^{20} cm^{-3} and a mobility of 86 cm^2/Vs. Slightly lower conductivities are obtained for a range of carrier concentrations and Ti contents. However, as the carrier mobility decreases with increasing Ti content, the highest conductivities are evidently observed for Ti contents up to 1 cat.%.

DISCUSSION

It is evident from the electrical measurements that the carrier concentration in Ti-doped In_2O_3 films is limited to values $<7.4 \times 10^{20}$ cm^{-3}, which is reached for Ti concentrations of 1 cat.% ($\approx 3 \times 10^{20}$ cm^{-3}). It is striking that, for a deposition temperature of 400 °C and for Ti contents <2 cat.%, the carrier concentrations of the co-sputtered films increase faster than the Ti content, resulting in carrier concentrations of up to two times the Ti concentration. A possible explanation for this observation is that the Ti atoms do not directly act as dopants inside the films but are rather forming precipitates and scavenge oxygen from the surrounding, thereby introducing oxygen vacancies in In_2O_3 as effective dopants.

The scavenging of oxygen is confirmed by analysis of the oxygen content of the films, which has been quantified by integrating the background subtracted core level intensities and normalization with respect to the atomic sensitivity factors.[32] The result is shown in Fig. 9. It is mentioned that such analysis is only reasonable if the measurements are performed *in situ*, without exposure of the samples to ambient conditions between deposition and XPS analysis. Exposure to air would cause adsorption of water, which would contribute to the oxygen signal.

As indicated by the open symbols in Fig. 9, the oxygen content of the films does not increase with the Ti content but rather stays constant within the experimental uncertainty. If the limitation of the carrier concentration is caused by oxygen interstitials, the oxygen content should increase with the Ti content as indicated by the dashed line in Fig. 9. Such an increase of the oxygen content with dopant concentration is, for example, observed for Sn doping. It is, therefore, clear that not all Ti atoms can occupy In lattice sites as substitutional Ti_{In} species. In this case, the Ti atoms would either act as donors with a Ti^{4+} oxidation state and every Ti atom exceeding the maximum carrier concentration would then have to be compensated by oxygen interstitials. A

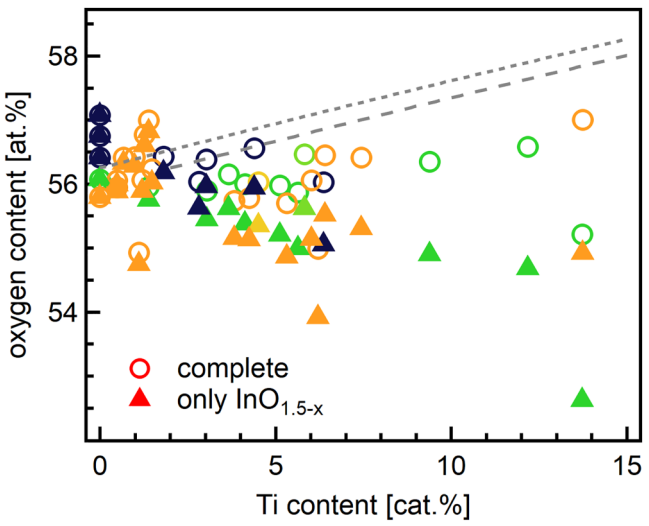

FIG. 9. Oxygen content of the co-sputtered In_2O_3 films determined from *in situ* XPS measurements. Open symbols correspond to extracted values and filled symbols to the oxygen content in the In_2O_3 part of the sample assuming that the films are a two-phase mixture of oxygen deficient In_2O_3 and TiO_2. The color of the symbols represents the deposition temperature and is the same as that used in the other figures. The dashed gray line indicates the expected trend of the oxygen content if all Ti atoms exceeding 2 cat.% would be compensated by interstitial oxygen species. The dotted line corresponds to the oxygen content if the films would be a two-phase mixture of stoichiometric In_2O_3 and TiO_2.

reduction of those Ti atoms that exceed the carrier limit to Ti^{3+} can also be ruled out from the Ti 2*p* XP spectra as these do not show significant amounts of Ti^{3+} (see Fig. 6). Hence, self-compensation and reduction of the dopant are ruled out as origin for the limitation of the carrier concentration of Ti-doped In_2O_3 films.

If Ti atoms are not occupying In sites, they likely form TiO_2 precipitates. These precipitates are not necessarily detected by XRD, as they are likely of nanometer extension and may also be amorphous. A direct determination of nanoscale TiO_2 precipitates might be possible by means of Raman spectroscopy. We have not been successful, however, to properly focus the laser on the transparent samples. Silicon substrates would be better suited for this purpose but have not been applied in this study. Assuming that the films consist of a homogeneously distributed two-phase mixture of In_2O_3 and TiO_2, the oxygen content in the In_2O_3 phase can be calculated from the overall oxygen content. As indicated by the filled symbols in Fig. 9, the calculated oxygen content in the In_2O_3 phase decreases by up to 2 % with increasing Ti content. The decrease of the oxygen content is likely specific to the used deposition method, as Ti is offered in a metallic form and may further reduce the oxygen content in the chamber by the sublimation pump effect.[29] It is mentioned that the concentration of oxygen is still higher than the values at which metallic In can be observed.

Explaining the achieved carrier concentrations by oxygen vacancies would be straightforward if every oxygen vacancy contributes two electrons to the free carrier concentration.[23,45,46] According to a combined study of *ab initio* defect calculations and electrical characterization of epitaxial In_2O_3 films in dependence of film thickness, it has been concluded that oxygen vacancies are deep donors, which cannot contribute such high equilibrium concentrations of electrons and that surface oxygen vacancies are the source of the carrier concentrations dominating for a film thickness of up to 150 nm.[47] The general gradient approximation in this study requires additional corrections of bandgaps and defect energy levels. In contrast, another *ab initio* study using hybrid functionals, where such corrections are usually not required, has revealed that oxygen vacancies are shallow defects in bulk In_2O_3.[46] The measured high carrier concentration for nominally undoped In_2O_3 films [see, e.g., Figs. 1 and 8(a)] corresponds well with a shallow nature of bulk oxygen vacancies. Additionally, with ≈300 nm thickness, the studied films are too thick to explain the number of free carriers by surface dopants.

If oxygen vacancies are the effective dopants in In_2O_3, the limitation of the carrier concentration is likely caused by neutralization of the oxygen vacancies according to

$$v_O^{\bullet\bullet} + 2e' \rightarrow v_O^{\times}. \quad (1)$$

It is then to be expected that nominally undoped In_2O_3 films containing the highest possible oxygen vacancy concentrations exhibit similar carrier concentrations as achieved in the present work with Ti doping (7×10^{20} cm^{-3}). We are, however, not aware of such high carrier concentrations of nominally undoped In_2O_3. The reason for this might be that it is quite difficult to reach such high concentration of oxygen vacancies experimentally, as it requires to control the oxygen partial pressure close to the stability limit of In_2O_3 at an oxygen chemical potential of $\mu(O) \approx -3.1$ eV.[40] This corresponds to an oxygen partial pressure of 10^{-35} bar at a typical processing temperature of 400 °C. One possibility to reach such low pO_2 is by reactive sputtering of In_2O_3 from metallic In targets. However, the process control would need to be extremely precise to avoid the formation of metallic In precipitates. The oxygen partial pressure might be easier to control with molecular beam epitaxy (MBE), but we are not aware that it has been tried explicitly to maximize the carrier concentrations of nominally undoped In_2O_3 films with this technique. Another complication arises as MBE grown films typically aim at epitaxial growth and employ Y-stabilized ZrO_2 (YSZ) substrates. YSZ is an excellent oxygen ion conductor and will affect the oxygen content in the deposited films.

Further credit for the interpretation of the data described above is provided by similar behavior reported for Ti-doped In_2O_3 bulk ceramics by Guilmeau *et al.*[11] In their case, saturation of the carrier concentration occurs at ≈4×10^{20} cm^{-3}. At low Ti concentration, the carrier concentration also increases faster than the Ti concentration. In the case of the bulk ceramics, x-ray diffraction clearly revealed the formation of an In_2TiO_5 secondary phase. The differences in maximum carrier concentration and secondary phase formation are likely due to different oxygen activity and synthesis temperature.

The formation of precipitates also explains the strong decrease of carrier mobility with increasing Ti content, which is evident from Fig. 8(b). The mobility decreases, although the number of ionized dopants, assumed to be equal to the number of free charge

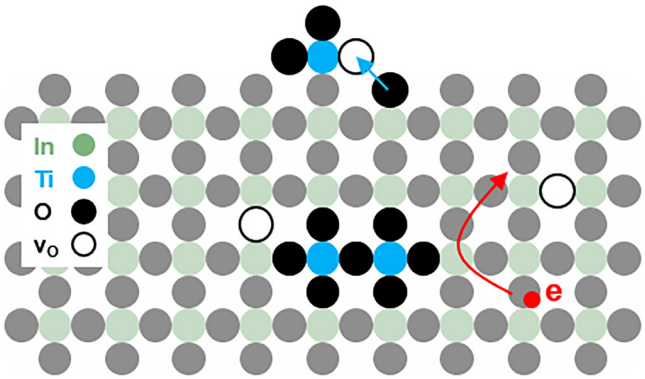

FIG. 10. Schematic representation of the process of deposition of titanium doped indium oxide. Oxygen from the substrate is consumed to form stable TiO_2 nuclei on the surface. The resulting film is suggested to consist of a two-phase mixture of crystalline In_2O_3 and nanoscopic neutral TiO_2 precipitates, which act as scattering centers for electrons. The mobile electrons are generated by oxygen vacancies.

carriers, does not decrease for Ti concentrations higher than 1 cat.%. Any precipitates would disturb the long-range order of the lattice and, therefore, lead to carrier scattering.

The suggested mechanism for doping of In_2O_3 thin films by Ti is schematically illustrated in Fig. 10. The formation of TiO_2 precipitates might be related to the high formation enthalpy of TiO_2 (−888.8 kJ/mol), which, per cation, is about twice that of In_2O_3 (−830.7 kJ/mol).[48] If this is true, formation of metallic precipitates is then also expected for other dopants whose oxides have high formation enthalpies. Therefore, we expect similar behavior for Zr as a dopant. This is consistent with the observation that In_2O_3 films doped with 2 wt. % Zr reach only slightly higher electron concentrations of 4.5×10^{20} cm^{-3} than films doped with 1 wt.% Zr (4.0×10^{20} cm^{-3}; see Fig. 1).

SUMMARY AND CONCLUSION

The properties of Ti-doped In_2O_3 films prepared by partial reactive co-sputtering—co-sputtering from ceramic In_2O_3 and metallic Ti targets—have been studied by means of *in situ* x-ray photoelectron spectroscopy and electrical measurements. XPS revealed the amount of Ti and oxygen in the films and no strong Ti surface segregation. No significant contributions of Ti^{3+} are observed. The oxygen content does not increase with the Ti content, which has to be expected if Ti dopants are compensated by oxygen interstitials or if the films are composed of a two-phase mixture of stoichiometric In_2O_3 and TiO_2. Together with the observation that the concentration of electronic carriers increases faster than the Ti concentration for low Ti content, it is concluded that electronic carriers are not generated by substitutional Ti_{In} donor defects but rather by oxygen vacancies, which are introduced by the scavenging of oxygen from Ti when forming TiO_2 precipitates. This implies that oxygen vacancies are shallow donors in bulk In_2O_3. While a direct determination of such precipitates is still outstanding, the suggested model concurs well with the saturation of electronic carrier concentrations at $\approx 7 \times 10^{20}$ cm^{-3}, which is reached at a Ti concentration of 1 cat.% ($\approx 3 \times 10^{20}$ cm^{-3}). Within this model, the limitation of the carrier concentration is caused by the neutralization of oxygen vacancies, occurring for Fermi energies inside the conduction band.

SUPPLEMENTARY MATERIAL

The supplementary material contains selected background subtractions of the Ti $2p_{3/2}$ photoelectron peak, additional XP survey, O 1*s*, In 3*d*, and Ti 2*p* core level spectra of Ti-doped In_2O_3 films prepared at room temperature, 200 °C, and 400 °C, and UV-VIS transmission spectra of Ti-doped In_2O_3 films grown at 400 °C

ACKNOWLEDGMENTS

The presented work has been supported by the German Research Foundation (DFG) within Project No. KL1225/9-1.

AUTHOR DECLARATIONS

Conflict of Interest

The authors have no conflicts to disclose.

Author Contributions

Ann-Katrin Emmerich: Data curation (equal); Investigation (equal); Writing – original draft (lead); Writing – review & editing (supporting). **Kim Alexander Creutz:** Data curation (supporting); Investigation (supporting); Supervision (lead). **Yaw-Yeu Cheng:** Data curation (equal); Investigation (equal). **Jean-Christophe Jaud:** Data curation (supporting); Investigation (supporting). **Andreas Hubmann:** Data curation (supporting); Investigation (supporting). **Andreas Klein:** Conceptualization (lead); Data curation (equal); Funding acquisition (lead); Supervision (supporting); Validation (equal); Writing – review & editing (lead).

DATA AVAILABILITY

The data that support the findings of this study are available from the corresponding author upon reasonable request.

REFERENCES

[1] *Handbook of Transparent Conductors*, edited by D. S. Ginley, H. Hosono, and D. C. Paine (Springer, New York, 2010).
[2] K. Ellmer, "Past achievements and future challenges in the development of optically transparent electrodes," Nat. Photonics **6**, 809 (2012).
[3] A. Walsh, J. L. F. D. Silva, S.-H. Wei, C. Körber, A. Klein, L. F. J. Piper, A. DeMasi, K. E. Smith, G. Panaccione, P. Torelli, D. J. Payne, A. Bourlange, and R. G. Egdell, "The nature of the bandgap in In_2O_3 revealed by first-principles calculations and x-ray spectroscopy," Phys. Rev. Lett. **100**, 167402 (2008).
[4] H. Ohta, M. Orita, M. Hirano, H. Tanji, H. Kawazoe, and H. Hosono, "Highly electrically conductive indium–tin–oxide thin films epitaxially grown on yttria-stabilized zirconia (100) by pulsed-laser deposition," Appl. Phys. Lett. **76**, 2740 (2000).
[5] N. Preissler, O. Bierwagen, A. T. Ramu, and J. S. Speck, "Electrical transport, electrothermal transport, and effective electron mass in single-crystalline In_2O_3 films," Phys. Rev. B **88**, 085305 (2013).

[6]O. Bierwagen and J. S. Speck, "Plasma-assisted molecular beam epitaxy of Sn-doped In_2O_3: Sn incorporation, structural changes, doping limits, and compensation," Phys. Stat. Sol. A **211**, 48 (2014).
[7]M. V. Frischbier, H. F. Wardenga, M. Weidner, O. Bierwagen, J. Jia, Y. Shigesato, and A. Klein, "Influence of dopant species and concentration on grain boundary scattering in degenerately doped In_2O_3 thin films," Thin Solid Films **614**, 62 (2016).
[8]I. Hamberg and C. G. Granqvist, "Evaporated Sn-doped In_2O_3 films: Basic optical properties and applications to energy-efficient windows," J. Appl. Phys. **60**, R123 (1986).
[9]E. Kobayashi, Y. Watabe, T. Yamamoto, and Y. Yamada, "Cerium oxide and hydrogen Co-doped indium oxide films for high-efficiency silicon heterojunction solar cells," Sol. Energy Mater. Sol. Cells **149**, 75 (2016).
[10]M. van Hest, M. S. Dabney, J. D. Perkins, D. S. Ginley, and M. P. Taylor, "Titanium-doped indium oxide: A high-mobility transparent conductor," Appl. Phys. Lett. **87**, 032111 (2005).
[11]E. Guilmeau, D. Bérardan, C. Simon, A. Maignan, B. Raveau, D. O. Ovono, and F. Delorme, "Tuning the transport and thermoelectric properties of In_2O_3 bulk ceramics through doping at In-site," J. Appl. Phys. **106**, 053715 (2009).
[12]Y. Meng, X.-L. Yang, H.-X. Chen, J. Shen, Y.-M. Jiang, Z.-J. Zhang, and Z.-Y. Hua, "A new transparent conductive thin film In_2O_3:Mo," Thin Solid Films **394**, 218 (2001).
[13]D. S. Bhachu, D. O. Scanlon, G. Sankar, T. D. Veal, R. G. Egdell, G. Cibin, A. J. Dent, C. E. Knapp, C. J. Carmalt, and I. P. Parkin, "Origin of high mobility in molybdenum-doped indium oxide," Chem. Mater. **27**, 2788 (2015).
[14]P. F. Newhouse, C. H. Park, D. A. Keszler, J. Tate, and P. S. Nyholm, "High electron mobility W-doped In_2O_3 thin films by pulsed laser deposition," Appl. Phys. Lett. **87**, 112108 (2005).
[15]T. Koida and M. Kondo, "High-mobility transparent conductive Zr-doped In_2O_3," Appl. Phys. Lett. **89**, 082104 (2006).
[16]T. Koida and M. Kondo, "Comparative studies of transparent conductive Ti-, Zr-, and Sn-doped In_2O_3 using a combinatorial approach," J. Appl. Phys. **101**, 063713 (2007).
[17]E. Kobayashi, Y. Watabe, and T. Yamamoto, "High-mobility transparent conductive thin films of cerium-doped hydrogenated indium oxide," Appl. Phys. Express **8**, 015505 (2015).
[18]T. Koida, H. Fujiwara, and M. Kondo, "Hydrogen-doped In_2O_3 as high-mobility transparent conductive oxide," Jpn. J. Appl. Phys. **46**, L685 (2007).
[19]T. Koida, Y. Ueno, and H. Shibata, "In_2O_3-based transparent conducting oxide films with high electron mobility fabricated at low process temperatures," Phys. Stat. Sol. A **215**, 1700506 (2018).
[20]G. Frank and H. Köstlin, "Electrical properties and defect model of tin-doped indium oxide layers," Appl. Phys. A **27**, 197 (1982).
[21]N. Yamada, I. Yasui, Y. Shigesato, H. Li, Y. Ujihira, and K. Nomura, "Donor compensation and carrier-transport mechanisms in tin-doped In_2O_3 films studied by means of conversion electron ^{119}Sn Mössbauer spectroscopy and Hall effect measurements," Jpn. J. Appl. Phys. **39**, 4158 (2000).
[22]G. B. González, T. O. Mason, J. P. Quintana, O. Warschkow, D. E. Ellis, J.-H. Hwang, J. P. Hodges, and J. D. Jorgensen, "Defect structure studies of bulk and nano-indium-tin oxide," J. Appl. Phys. **96**, 3912 (2004).
[23]S. Lany and A. Zunger, "Dopability, intrinsic conductivity, and nonstoichiometry of transparent conducting oxides," Phys. Rev. Lett. **98**, 045501 (2007).
[24]P. Ágoston, C. Körber, A. Klein, M. J. Puska, R. M. Nieminen, and K. Albe, "Limits for *n*-type doping in In_2O_3 and SnO_2: A theoretical approach by first-principles calculations using hybrid-functional methodology," J. Appl. Phys. **108**, 053511 (2010).
[25]W. Walukiewicz, "Intrinsic limitations to the doping of wide-gap semiconductors," Physica B **302–303**, 123 (2001).
[26]A. Klein, K. Albe, N. Bein, O. Clemens, K. A. Creutz, P. Erhart, M. Frericks, E. Ghorbani, J. P. Hofmann, B. Huang, B. Kaiser, U. Kolb, J. Koruza, C. Kübel, K. N. S. Lohaus, J. Rödel, J. Rohrer, W. Rheinheimer, R. A. D. Souza, V. Streibel, A. Weidenkaff, M. Widenmeyer, B.-X. Xu, and H. Zhang, "The Fermi energy as common parameter to describe charge compensation mechanisms: A path to Fermi level engineering of oxide electroceramics," J. Electroceram. **51**, 147 (2023).
[27]D. Harra, "Review of sticking coefficients and sorption capacities of gases on titanium films," J. Vac. Sci. Technol. **13**, 471 (1976).
[28]A. Zangwill, *Physics at Surfaces* (Cambridge University Press, Cambridge, 1988).
[29]A. Gupta and J. Leck, "An evaluation of the titanium sublimation pump," Vacuum **25**, 362 (1975).
[30]K. Jousten, *Handbook of Vacuum Technology* (Wiley-VCH, Weinheim, 2016).
[31]A. Klein, "Transparent conducting oxides: Electronic structure–property relationship from photoelectron spectroscopy with *in situ* sample preparation," J. Am. Ceram. Soc. **96**, 331 (2013).
[32]J. Moulder and J. Chastain, *Handbook of X-ray Photoelectron Spectroscopy: A Reference Book of Standard Spectra for Identification and Interpretation of XPS Data* (Physical Electronics Division, Perkin-Elmer Corporation, 1992).
[33]M. V. Hohmann, A. Wachau, and A. Klein, "*In situ* Hall effect and conductivity measurements of ITO thin films," Solid State Ion. **262**, 636 (2014).
[34]H. Wardenga, M. V. Frischbier, M. Morales-Masis, and A. Klein, "*In situ* Hall effect monitoring of vacuum annealing of In_2O_3:H thin films," Materials **8**, 561 (2015).
[35]J. J. Yeh and I. Lindau, "Subshell photoionization cross sections," At. Data Nucl. Data Tables **32**, 1 (1985).
[36]C. Körber, V. Krishnakumar, A. Klein, G. Panaccione, P. Torelli, A. Walsh, J. L. F. D. Silva, S.-H. Wei, R. G. Egdell, and D. J. Payne, "Electronic structure of In_2O_3 and Sn-doped In_2O_3 by hard x-ray photoemission spectroscopy," Phys. Rev. B **81**, 165207 (2010).
[37]Y. Gassenbauer, R. Schafranek, A. Klein, S. Zafeiratos, M. Hävecker, A. Knop-Gericke, and R. Schlögl, "Surface states, surface potentials, and segregation at surfaces of tin-doped In_2O_3," Phys. Rev. B **73**, 245312 (2006).
[38]S. P. Harvey, T. O. Mason, Y. Gassenbauer, R. Schafranek, and A. Klein, "Surface vs bulk electronic/defect structures of transparent conducting oxides. Part I. Indium oxide and ITO," J. Phys. D.: Appl. Phys. **39**, 3959 (2006).
[39]F. Rüggeberg and A. Klein, "The In_2O_3/CdTe interface: A possible contact for thin film solar cells?," Appl. Phys. A **82**, 281 (2006).
[40]P. Ágoston and K. Albe, "Thermodynamic stability, stoichiometry and electronic structure of bcc-In_2O_3 surfaces," Phys. Rev. B **84**, 045311 (2011).
[41]V. Golovanov, M. A. Mäki-Jaskari, T. T. Rantala, G. Korotcenkov, V. Brinzari, A. Cornet, and J. Morante, "Experimental and theoretical studies of indium oxide gas sensors fabricated by spray pyrolysis," Sens. Actuators B: Chem. **106**, 563 (2005).
[42]M. Batzill, K. Katsiev, J. M. Burst, U. Diebold, A. M. Chaka, and B. Delley, "Gas-phase-dependent properties of SnO_2 (110), (100), and (101) single-crystal surfaces: Structure, composition, and electronic properties," Phys. Rev. B **72**, 165414 (2005).
[43]A. Hubmann, "Doped indium oxide: Surface potentials, electronic and optical properties," Ph.D. thesis (Technical University of Darmstadt, 2021).
[44]With a density of $7.18\,g/cm^3$, the In concentration in In_2O_3 corresponds to $3.09 \times 10^{22}\,cm^{-3}$.
[45]P. Ágoston, P. Erhart, A. Klein, and K. Albe, "Geometry, electronic structure and thermodynamic stability of intrinsic point defects in indium oxide," J. Phys.: Condens. Matter **21**, 455801 (2009).
[46]P. Ágoston, K. Albe, R. M. Nieminen, and M. J. Puska, "Intrinsic *n*-type behavior in transparent conducting oxides: A comparative hybrid-functional study of In_2O_3, SnO_2, and ZnO," Phys. Rev. Lett. **103**, 245501 (2009).
[47]S. Lany, A. Zakutayev, T. O. Mason, J. F. Wager, K. R. Poeppelmeier, J. D. Perkins, J. J. Berry, D. S. Ginley, and A. Zunger, "Surface origin of high conductivities in undoped In_2O_3 thin films," Phys. Rev. Lett. **108**, 016802 (2012).
[48]*CRC Handbook of Chemistry and Physics*, 85th ed., edited by D. R. Lide (CRC Press, Boca Raton, FL, 2005).